Chemical Physics Letters 584 (2013) 142–146

Contents lists available at ScienceDirect

Chemical Physics Letters

journal homepage: www.elsevier.com/locate/cplett

CVD synthesis of mono- and few-layer graphene using alcohols at low hydrogen concentration and atmospheric pressure

Jessica Campos-Delgado [a,*], Andrés R. Botello-Méndez [b], Gerardo Algara-Siller [c], Benoit Hackens [b], Thomas Pardoen [d], Ute Kaiser [c], Mildred S. Dresselhaus [e], Jean-Christophe Charlier [b], Jean-Pierre Raskin [a]

[a] Institute of Information and Communication Technologies, Electronics and Applied Mathematics, Université catholique de Louvain, Louvain-la-Neuve 1348, Belgium
[b] Institute of Condensed Matter and Nanosciences, Nanoscopic Physics, Université catholique de Louvain, Louvain-la-Neuve 1348, Belgium
[c] Central Facility of Electron Microscopy, Ulm University, Ulm 89073, Germany
[d] Institute of Mechanics, Materials and Civil Engineering, Université catholique de Louvain, Louvain-la-Neuve 1348, Belgium
[e] Department of Electrical Engineering and Computer Science, Massachusetts Institute of Technology, Cambridge, MA 02139, USA

ARTICLE INFO

Article history:
Received 4 July 2013
In final form 12 August 2013
Available online 20 August 2013

ABSTRACT

An original and easy route to produce mono-, bi- and tri-layer graphene is proposed using the chemical vapor deposition technique. The synthesis is carried out at atmospheric pressure using liquid precursors, copper as catalyst, and a single gas injection line consisting of a very diluted mixture of H_2 in Argon (H_2: 5%). Two different alcohols are investigated as possible sources of carbon: 2-phenylethanol and ethanol. The characterization of the samples with SEM, TEM and Raman spectroscopy confirms the presence of graphene on top of copper, and yields a detailed picture of the structure of the produced graphene layers.

1. Introduction

The graphene revolution has induced a clear demand on alternative production routes to the mechanical exfoliation technique that popularized it in 2004 [1]. Although the ease of the exfoliation technique allowed its fast implementation in research laboratories worldwide, the low throughput represented a serious drawback in view of industrial applications. The epitaxial growth of graphene on SiC [2] and the thermal decomposition of hydrocarbons on highly crystalline metal surfaces like Ru(0001) [3] and Ir(111) [4] have been explored to synthesize graphene films. Without doubt the most popular alternative production route saw the light in 2009 when the chemical vapor deposition (CVD) synthesis of graphene was reported using polycrystalline nickel as a catalyst and methane as a carbon source [5,6]. Later that same year, Ruoff's group published the synthesis using commercial copper foils [7] and elucidated the different mechanisms involved in the synthesis either with Ni or Cu using carbon isotope labeling and Raman spectroscopy [8]. The synthesis technique relies on the decomposition of methane at ~1000 °C and low pressure and its deposition on the metal catalysts. In the case of Ni, where C solubility is high, the mechanism of growth is through the segregation and precipitation of C once Ni is cooled down; in contrast, C solubility in Cu is low and the growth is mediated by surface adsorption [8]. Carbon in the three phases (gas, liquid and solid) has been used to produce graphene catalyzed by copper: as a gas in methane [5–7] and ethylene [4]; as a solid in polymers (poly methyl methacrylate, PMMA), sugar [9] and, basically, anything solid containing carbon [10]; and as a liquid in hexane, benzene and alcohols [11–13]. The above listed precursors are used in experiments at low pressure conditions (mTorr) and generally gases of 100% concentration of Ar, CH_4 and H_2 are involved in the synthesis, which require a sophisticated set-up with pumping system, the availability of 2–3 gas lines, several flow meters, and proper stainless steel piping for H_2 and CH_4 for safety reasons, since both gases are highly flammable. Recent communications have reported on the synthesis of graphene at atmospheric pressures [14,15]. Dong and coauthors [14] used ethanol and pentane as carbon sources and although no low pressure is involved, two gas lines: Ar and Ar–H_2, are needed and the H_2 concentration is rather high (20%). Vlassiouk and co-workers [15] use a very diluted mixture hydrogen during synthesis (2.5%), however, methane is still preferred as source of carbon which implies the need of two gas inlets.

The CVD synthesis of large-area bi-layer graphene has been addressed by several groups in the literature: S. Lee et al. [16] were able to grow bi-layer graphene from CH_4 at low pressures, K. Yan et al. [17] use a two-step process to produce Bernal stacked bi-layer graphene using low pressures and CH_4 and H_2, while J.K. Wassei et al. [18] explore the production of bilayer graphene with ethane (C_2H_6) and H_2 at low pressures.

Raman spectroscopy constitutes a powerful tool to characterize graphene since it allows the identification of single layer graphene thanks to its unique fingerprint, where the G′ band

* Corresponding author.
E-mail address: jessica.campos@uclouvain.be (J. Campos-Delgado).

0009-2614/$ - see front matter © 2013 Elsevier B.V. All rights reserved.
http://dx.doi.org/10.1016/j.cplett.2013.08.031

($\sim$2700 cm^{-1}) presents a very large intensity compared to that of the G band ($\sim$1580 cm^{-1}) exhibiting line width values of around 30 cm^{-1}. In addition, this spectroscopy technique allows as well the quantification of the number of layers in Bernal-stacked few-layer graphene [19].

The present Letter presents a methodological advantage to the synthesis of graphene by atmospheric pressure CVD (APCVD) which is, by itself, a simplification of more common CVD setups. Current CVD methods reported in the literature [5–15] rely on the availability of vacuum systems, several gas input lines to deliver Ar, H_2 and CH_4 (or at least two of the above) to the CVD reactor. Besides, safety hazards should be considered along with the use of flammable gases like CH_4 and H_2 or even Ar–H_2 mixtures with high H_2 concentration. Our approach relies on a simple ambient pressure set-up equipped with a single gas inlet (a gas mixture of Ar–H_2 with a very diluted concentration of H_2 (5%)) and the use of alcohols as carbon precursors. The produced carbon-based materials have been characterized using a combination of tools including scanning and transmission electron microscopy, and Raman spectroscopy.

2. Materials and methods

2.1. Synthesis

We use commercial Cu foils of 25 μm in thickness purchased from Advent Research Materials Ltd with purity of 99.9%. The received foils of 0.025 × 100 × 100 mm were cut into pieces of 1 cm^2 and then mildly cleaned in acetone and isopropyl alcohol. The foils were fit to a combustion boat further placed inside an alumina tube in a tubular furnace. As a carbon source we used two alcohols: 2-phenylethanol and ethanol (Sigma–Aldrich). A diagram illustrating the set-up is depicted in Figure 1. This configuration allows us to split one gas inlet in two paths by means of glass valves: one for heating, annealing and cooling down (P1); and a second one for the actual graphene growth (P2). The synthesis temperature is set to 980 or 990 °C in the tubular furnace; during heating, the Ar–H_2 (5% of H_2) flow is tuned to 0.2 l/min through P1. Once the furnace has reached the target temperature we perform an annealing of the Cu during 20–30 min. Right after we tune the flow to the desired rate for growth, we allow the flow to pass through the alcohol container (P2) for the graphene growth, and the time is varied depending on the precursor. Through this growth time the container is placed on a water bath with boiling water. Maintaining the flow rate, we redirect the flux to P1 and we perform a 10 min annealing of the sample. We have found that this annealing step increases the quality of the graphene film, proved by a decrease on the D band signal in the Raman spectra (results not shown here). After this time the flow is decreased to 0.2 l/min and the furnace is turned off to cool down to room temperature. In our experiments the parameters to be varied are: synthesis temperature (980 or 990 °C), time of growth, and flow rate; these two last parameters allow a control on the amount of carbon delivered to the system during the experiment.

2.2. Transfer

After synthesis the copper foil is covered with graphene on both surfaces. To further characterize the material we transfer the graphene films to Si/SiO_2 substrates. The material is transferred using the following method: (1) a film of poly(methyl methacrylate) (PMMA, 950 K molecular weight, 2% in anisole) is drop-coated on one side of the film, (2) the uncoated side is exposed to O_2 plasma to remove the protective graphene film, (3) the copper foil-graphene-PMMA is left overnight in a $FeCl_3$ solution with the copper area in contact with the solution and, (4) the graphene/PMMA film is scooped out of the $FeCl_3$ etchant solution, rinsed in deionized water three times and put in contact with the target Si/SiO_2 substrate, (5) a second film of PMMA is drop coated and left to dry, (6) finally the substrate is immersed in warm acetone (40 °C) to dissolve the PMMA and rinsed with isopropyl alcohol.

2.3. Raman spectroscopy

Micro-Raman spectroscopy measurements have been performed with laser excitation energies in the range 2.16–2.54 eV at room temperature for 10 s with laser powers of $\sim$2.3 mW. The samples were analyzed in the backscattering configuration using a 100× objective lens. For convenience, measurements were made with five different laser energies: argon (2.54, 2.47, 2.41 eV), YAG (2.33 eV) and Rhodamine dye (2.16 eV). Maps were recorded using a motorized stage with a step size of 0.3 μm and E_{laser} = 2.33 eV.

2.4. Electron microscopy

Scanning electron microscopy has been carried out using a FEG Zeiss Ultra55 microscope operated at 5 kV. TEM imaging has been carried out by transferring our materials to 200 mesh Au grids (Quantifoil), following the method reported in Reference [20]. For TEM imaging we used an image-side aberration corrected FEI TITAN 80–300 microscope operated at 80 kV with a spherical aberration of 0.02 mm at Scherzer defocus.

3. Results and discussion

Scanning electron microscopy and Raman spectroscopy are first used to investigate the produced graphene samples. Figure 2

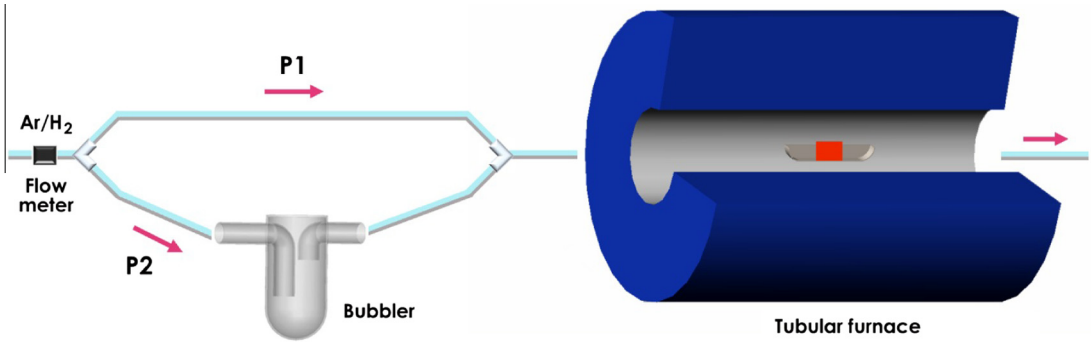

Figure 1. Diagram of the configuration used in the experiment. A single gas inlet is split into two paths (P1 and P2) using glass ware. During heating/annealing/cooling, gas is passed through P1; while for graphene growth, gas flows through P2 and bubbles in the alcohol container. Inside the tubular furnace a combustion boat is placed in the center containing a piece of copper foil.

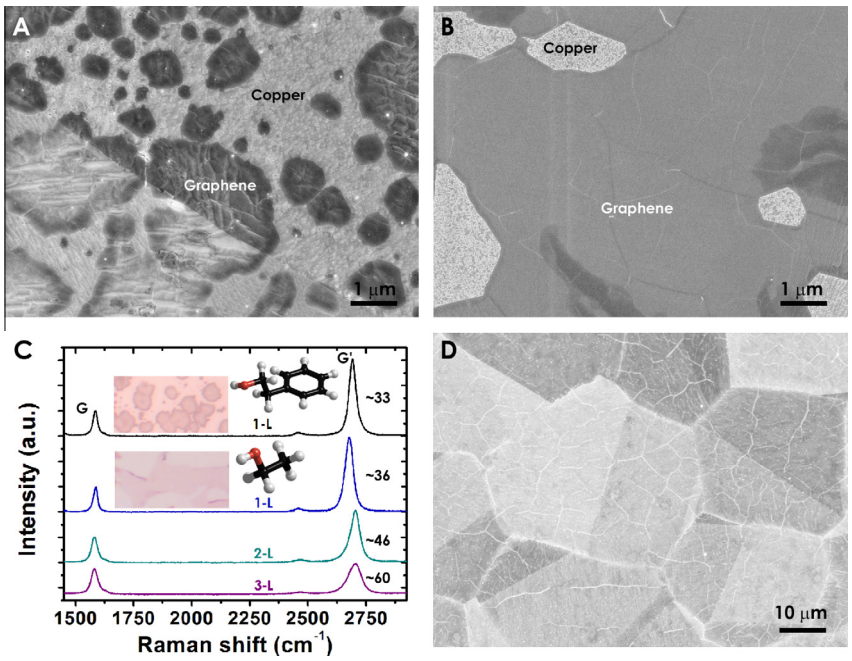

Figure 2. SEM micrographs of mono-layer samples produced with (A) 2-phenylethanol and (B) ethanol. Both the Cu substrate and the graphene are identified by labels. (C) Representative Raman spectra of mono-(1-L: black and blue curves for 2-phenylethanol and ethanol, respectively), bi-(2-L: green curve), and tri-(3-L: purple curve) layer graphene. Ball and stick models of the molecules are included for illustration: black balls represent carbon atoms, white balls stand for hydrogen and red ones for oxygen. The numbers at the right of the G′ bands represent the FWHM of the respective single Lorentzian fits. The insets are optical micrographs of the transferred single-layer materials. (D) SEM image of a Cu substrate uniformly covered of bi-layer graphene synthesized with ethanol at 980 °C. (For interpretation of the references to colour in this figure legend, the reader is referred to the web version of this article.)

shows typical low magnification SEM images of samples synthesized using 2-phenylethanol at 980 °C during 5 min (Figure 2A) and using ethanol at 990 °C during 10 s (Figure 2B) with flow rates of 1 l/min and 0.88 l/min, respectively. The large copper grains and graphene areas partially covering these grains are visible. In these images the typical graphene wrinkles, due to the thermal expansion coefficient mismatch between graphene and copper [21] (negative/positive thermal expansion coefficients, respectively), are evident. Raman spectroscopy spectra of both transferred samples are plotted in Figure 1C. Optical microscopy images of these transferred materials to Si/SiO_2 recorded at 100× are also included (Figure 2C insets). Raman spectroscopy confirmed that the light-contrasted areas consist of mono-layer graphene with typical values for the full width at half maximum (FWHM) of the G′ band of 30–36 cm^{-1} and $I_{G'}/I_G$ ratios of ~3. Although, monolayer graphene can be produced using both precursors, our results suggest that using 2-phenylethanol the average graphene-grain sizes are islands typically of 2 × 2 μm, while for ethanol larger domains of single-layer were observed (10 × 10 μm).

In order to obtain larger coverage using alcohols, synthesis parameters were changed. Consequently, a clear improvement in the coverage area was thus observed, as well as an increase in the number of layers present in the samples. In general we obtain better results with ethanol (i.e., better coverage, layer continuity and faster synthesis) than with 2-phenylethanol. In figure 2C spectra of double and triple layer samples produced with ethanol are also plotted. The optimal conditions for large coverage of bi-layer graphene are: ethanol as precursor at 980 °C for 10 s with a flow rate of 1 l/min. Longer growth times and higher flow rates result in more carbon deposition and hence more layers.

Raman measurements using five different laser excitation wavelengths 574, 532, 514, 501 and 488 nm (2.16, 2.33, 2.41, 2.47 and 2.54 eV, respectively), were performed on a uniformly-covered graphene sample synthesized at 980 °C using ethanol as precursor (Figure 2D). The corresponding spectra are presented in Figure 3A. We can easily notice the large intensities of the G′ bands (~2700 cm^{-1}), with average FWHM of 50 cm^{-1} according to our Lorentzian fittings. The dispersive behavior of the D (~1350 cm^{-1}) and G′ bands can be observed in Figure 3A, where insets to these bands are also illustrated. We found linear relations between the positions of the D and G′ bands (ω_D and $\omega_{G'}$, respectively) and the laser excitation energy (E_{laser}), this dispersive behavior is consistent with the double resonance (DR) theory [22]. In order to quantify these frequency dependences on laser energy, the plotted spectra were fitted with single Lorentzians and quantitative data related to the above mentioned energy dependences was further extracted.

In Figure 3B, the frequency positions of the main carbon bands are plotted as a function of laser excitation energy. From these data, the frequency-dependent slopes on E_{laser} were estimated for both the D and G′ bands: $\partial\omega_D/\partial E_{laser} \approx 39\ cm^{-1}/eV$ and $\partial\omega_{G'}/\partial E_{laser} \approx 85\ cm^{-1}/eV$. The present value of $\partial\omega_{G'}/\partial E_{laser}$ is very close to that of exfoliated monolayer graphene [23] (88 cm^{-1}/eV). In the same graph, the energy dependence of the intensity of the D band appears plotted as the I_D/I_G ratio (hexagons linked to the right hand Y-axis). This ratio decreases linearly with E_{laser}, as expected from DR theory. In order to evaluate the sample homogeneity, Raman spectroscopy maps were performed on an area of 18 × 18 μm^2. The G′ band intensity map is plotted in Figure 3C; confirming the layer homogeneity of the sample within the measured area by observing the small variation of intensity. The average value of the $I_{G'}/I_G$ ratio is 2 and the average FWHM of the G′ band is 55 cm^{-1}, as it can be appreciated in Figure 3D where two spectra extracted from the map are plotted, the inset shows the optical image of the area measured.

According to previous reports on CVD-grown graphene, the stacking of bi-layers is not AB-type but rather a random stack with uncontrolled rotational angles [5,7]. Indeed, such a random stacking is reflected in the Raman spectra since CVD bi-layer graphene does not reproduce the four-component G′ feature of Bernal

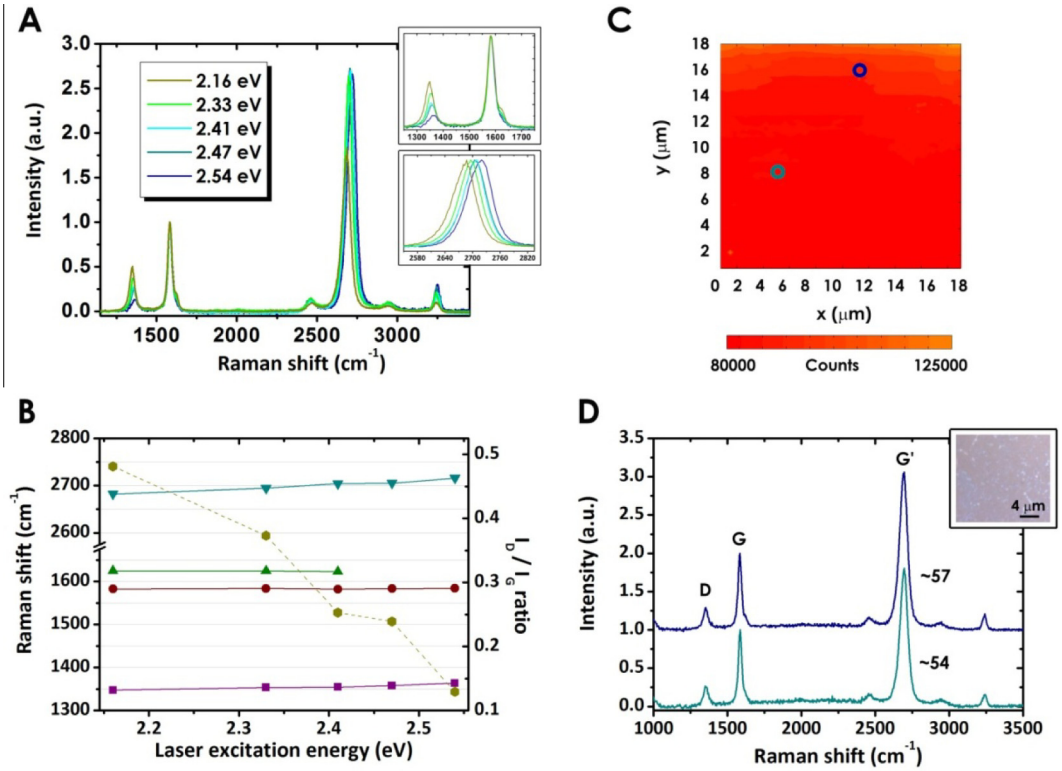

Figure 3. Bi-layer samples synthesized at 980 °C using ethanol as precursor. (A) Typical Raman spectra recorded with five different laser excitation energies (2.16, 2.33, 2.41, 2.47 and 2.54 eV). The upper inset presents an amplification of the D and G bands region, while the lower inset zooms in the high frequency region where the intensity of the G′ band has been normalized to 1 to visualize the energy dependent frequency shifts. (B) Energy dependence of the frequency positions for the D, G, D′ and G′ bands (rectangles, circles, triangles and inversed triangles, respectively, linked to the left hand *Y*-axis) and of the I_D/I_G ratios of the spectra presented in A (hexagons, dashed line, linked to the right hand *Y*-axis). (C) G′ band intensity map (E_{laser} = 2.33 eV). (D) Spectra extracted from the map at the corresponding spots highlighted by circles in C (intensities have been normalized to the G band). The numbers at the right of the G′ bands represent the FWHM of the respective single Lorentzian fits. The inset corresponds to the optical image of the region mapped in C.

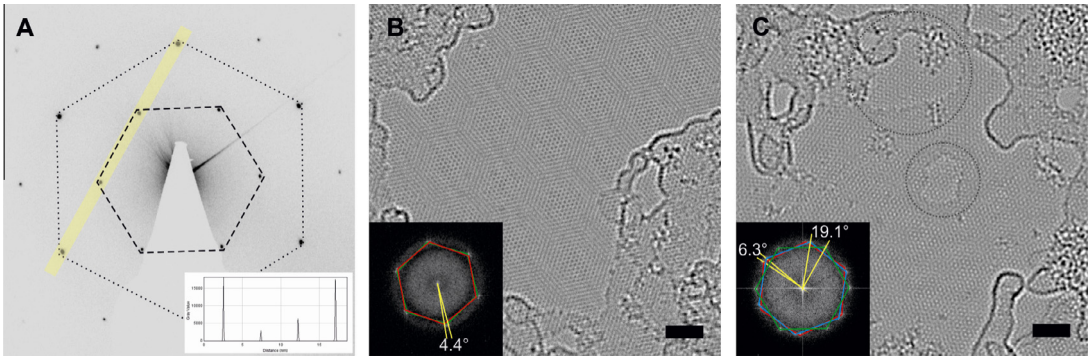

Figure 4. (A) Diffraction pattern obtained from a random area of an ethanol-derived sample. The dashed hexagon circumscribes the {10–10} type reflections (2.13 Å) of graphene and the dotted hexagon the {11–20} type reflections (1.23 Å). A profile plot, right down inset, taken along the yellow line shows that the sample at this position is bilayer graphene by the intensity difference between reflections. (B) HRTEM image of bilayer graphene showing a Moiré pattern. In the lower left corner the inset represents the FFT (Fast Fourier Transform) of the image. The green and red hexagons show the mismatch between reflections of the two layers with an angle of 4.4 degrees. (C) HRTEM image of triple layer graphene, where the areas circumscribed by grey circles point out a Moiré pattern produced only by two layers. The inset shows the FFT of the image, the vertices of the red, blue and green hexagons point to the corresponding reflections for each layer. In yellow the angles between reflections. Scale bars 2 nm. (For interpretation of the references to colour in this figure legend, the reader is referred to the web version of this article.)

stacked graphene exfoliated from HOPG (which arises from the splitting of the electronic bands in bi-layer as compared to mono-layer graphene). Instead, the G′ band of CVD bi-layer graphene would present a lower intensity and a larger line width, relative to the same Raman features in monolayer graphene. The large width of the G′ bands, the depletion of their intensities with respect to the G band observed in our measurements, and the $\partial\omega_{G'}/\partial E_{laser}$ value close to that of graphene suggest the presence of two largely decoupled layers of graphene (see Figure 3A and D).

This conclusion was confirmed by HRTEM and electron diffraction studies of the samples produced with ethanol at 980 °C (Figure 4). The electron diffraction spectrum of a random area of thismaterial reveals the main reflections of the honeycomb lattice of graphene (see Figure 4A). The dashed hexagon circumscribes

the 2.13 Å reflections and the dotted one the 1.23 Å reflections. The inset is a line profile plot taken along the yellow line, confirming that the sample in this region is bilayer graphene [24].

Figures 4B and C illustrate TEM images of randomly selected areas where bi- and tri- layer graphene, respectively. Randomly stacked graphene layers are again evident from the Moiré patterns that appear in the high resolution images (Figure 4B). The reciprocal space correspondence (Fast-Fourier Transform, FFT) of this image allows us to verify the presence of two layers of graphene and to quantify the rotational angle between them, which is estimated to be around 4.4°. During these TEM observations, randomly stacked tri-layer graphene was also observed (Figure 4C).

4. Conclusions

In this report, mono-, bi- and tri- layer graphene samples are synthesized using alcohol precursors at atmospheric pressure and using a single gas inlet of an Ar–H_2 mixture with a very low concentration of H_2 (5%). Using various characterization techniques, the bi- and tri- layer graphene films are found to be not strongly coupled, displaying random rotational angles between the stacked layers (HRTEM Moiré patterns). Indeed, using five different laser excitation energies, Raman scattering measurements of bi-layer graphene, demonstrate that the dispersion of the G′ bands is similar to that of exfoliated monolayer graphene, confirming again a strong decoupling between the layers. The ease of implementation of this synthesis method could represent an easy and cheap procedure to scale up and tune graphene production.

Acknowledgements

J.C.D. deeply thanks Fernando Aguilera for artwork assistance and David Spote for technical guidance. We acknowledge the technical assistance of Marc Sinnaeve, Andre Crahay, Augustin Dutu, Miloud Zitout, G. Dresselhaus and Thomas Hirschmann. J.C.D. thanks the FNRS and CONACyT for funding. M.S.D. acknowledges support from NSF DMR-100417. J.C.D, A.R.B.M, M.S.D and J.C.C are indebted to the MIT-UCL Seed Fund collaboration. A.R.B.M. and J.-C.C. acknowledge support from FNRS of Belgium. This Letter is directly connected to the ARC 'Graphene StressTronics' project (Convention No11/16-037) sponsored by the Communauté Française de Belgique. G.A.S acknowledges the support of CONACyT-DAAD scholarship.

References

[1] K.S. Novoselov et al., Science 306 (2004) 666.
[2] C. Berger et al., Science 312 (2006) 1191.
[3] S. Marchini, S. Günther, J. Wintterlin, Phys. Rev. B 76 (2007) 075429.
[4] J. Coraux, A.T. N'Diaye, C. Busse, T. Michely, Nano Lett. 8 (2008) 565.
[5] A. Reina et al., Nano Lett. 9 (2009) 30.
[6] K.S. Kim et al., Nature 457 (2009) 706.
[7] X. Li et al., Science 324 (2009) 1312.
[8] X. Li, W. Cai, L. Colombo, R.S. Ruoff, Nano Lett. 9 (2009) 4268.
[9] Z. Sun, Z. Yan, J. Yao, E. Beitler, Y. Zhu, J.M. Tour, Nature 468 (2010) 549.
[10] G. Ruan, Z. Sun, Z. Peng, J.M. Tour, ACS Nano 5 (2011) 7601.
[11] A. Srivastava et al., Chem. Mater. 22 (2010) 3457.
[12] L. Zhancheng et al., ACS Nano 5 (2011) 3385.
[13] A. Guermoune et al., Carbon 49 (2011) 4204.
[14] X. Dong et al., Carbon 49 (2011) 3672.
[15] I. Vlassiouk, P. Fulvio, H. Meyer, N. Lavrik, S. Dai, P. Datskos, S. Smirnov, Carbon 54 (2013) 58.
[16] S. Lee, K. Lee, Z. Zhong, Nano Lett. 10 (2010) 4702.
[17] K. Yan, H. Peng, Y. Zhou, H. Li, Z. Liu, Nano Lett. 11 (2011) 1106.
[18] J.K. Wassei, M. Mecklenburg, J.A. Torres, J.D. Fowler, B.C. Regan, R.B. Kaner, B.H. Weiller, Small 8 (2012) 1415.
[19] A.C. Ferrari et al., Phys. Rev. Lett. 97 (2006) 187401.
[20] R.S. Pantelic et al., J. Struct. Biol. 174 (2011) 234.
[21] Y. Zhang et al., ACS Nano 5 (2011) 4014.
[22] R. Saito et al., New J. Phys. 5 (2003) 157.1.
[23] D.L. Mafra et al., Phys. Rev. B 76 (2007) 233407.
[24] J. Meyer, A. Geim, M. Katsnelson, K. Novoselov, D. Obergfell, S. Roth, C. Girit, A. Solid State Commun. 143 (2007) 101.